

Tomography of zero-energy end modes in topological superconducting wires

A. A. Aligia,^{1,2,3} D. Pérez Daroca,^{4,3} and Liliana Arrachea^{5,3}

¹Centro Atómico Bariloche, Comisión Nacional de Energía Atómica, 8400 Bariloche, Argentina

²Instituto Balseiro, Comisión Nacional de Energía Atómica, 8400 Bariloche, Argentina

³Consejo Nacional de Investigaciones Científicas y Técnicas, 1025 CABA, Argentina

⁴Gerencia de Investigación y Aplicaciones, Comisión Nacional de Energía Atómica, 1650 San Martín, Buenos Aires, Argentina

⁵International Center for Advanced Studies, Escuela de Ciencia y Tecnología, Universidad Nacional de San Martín, 25 de Mayo y Francia, 1650 Buenos Aires, Argentina

(Dated: October 2, 2020)

We characterize the Majorana zero modes in topological hybrid superconductor-semiconductor wires with spin-orbit coupling and magnetic field, in terms of generalized Bloch coordinates φ, θ, δ , and analyze their transformation under SU(2) rotations. We show that, when the spin-orbit coupling and the magnetic field are perpendicular, φ and δ are universal in an appropriate coordinate system. We use these geometric properties to explain the behavior of the Josephson current in junctions of two wires with different orientations of the magnetic field and/or the spin-orbit coupling. We show how to extract from there, the angle θ , hence providing a full description of the Majorana modes.

Introduction. Topological superconductors host Majorana zero modes (MZMs) localized at the edges of the system [1, 2]. A significant effort is invested in the detection and manipulation of these states, because of their potential application for implementing topological quantum computation [3, 4]. Quantum wires with spin-orbit coupling (SOC), proximity-induced s-wave superconductivity and a magnetic field having a component perpendicular to the direction of the SOC [1, 6], are one of the most prominent systems. Several experimental works investigated realizations of this platform for topological superconductivity in wires of InAs [7–12].

The existence of MZMs leads to signatures in the behavior of the Josephson current. In the ac case, the periodicity as a function of the phase bias ϕ is 4π , in contrast to the 2π one of the ordinary superconductors. This feature is common to the non-time reversal invariant, [1, 13–36] and time-reversal invariant [37–48] families.

In the topological superconducting phase of the quantum wires proposed in Refs. [1, 6] the zero modes have a non-trivial spin texture [49–51]. A naive expectation suggests MZMs polarized at both ends of the wire along a direction determined by the magnetic field and the SOC. The explicit calculation of the spin density from the exact solution of the model Hamiltonian shows that the zero modes also have magnetization components perpendicular to the magnetic field and the spin-orbit axis. Remarkably, for perpendicular magnetic field and SOC, the components of the spin polarization perpendicular to the magnetic field are also perpendicular to the SOC and have opposite signs at the two ends of the wire [1, 49].

In the present work we introduce a geometrical characterization of the MZMs in terms of their Bloch coordinates φ, θ associated to the spin orientation and a phase δ . We denote these three parameters as generalized Bloch coordinates (GBC). We study the model introduced in Refs. [1, 6]. We show that, when the magnetic field and the SOC are perpendicular, there exist an *easy coordinate frame* (ECF) where φ and δ are universal and can be exactly calculated by means of symmetry

arguments, up to a sign that can be obtained from the solution in particular limits. We present a low-energy effective Hamiltonian to describe the MZMs in Josephson junctions and show that the angle θ can be inferred from the behavior of the Josephson current in suitable designed junctions. Hence, the combination of geometric properties along with the information of the Josephson current enables a full tomography of the MZMs.

Model for the wires. We consider a lattice version of the model for topological superconducting wires introduced in Refs. [1, 6], with arbitrary orientations of the magnetic field and SOC [52, 53]. The corresponding Hamiltonian is $H_w = H_0 + H_\Delta$, with

$$H_0 = \sum_{\ell} \mathbf{c}_{\ell}^{\dagger} (-t \sigma_0 - i \vec{\lambda} \cdot \vec{\sigma}) \mathbf{c}_{\ell+1} + \text{H.c.} \quad (1)$$

$$- \sum_{\ell} \mathbf{c}_{\ell}^{\dagger} (\vec{B} \cdot \vec{\sigma} + \mu \sigma_0) \mathbf{c}_{\ell}, \quad H_{\Delta} = \Delta \sum_{\ell} c_{\ell\uparrow}^{\dagger} c_{\ell\downarrow} + \text{H.c.},$$

where ℓ labels sites of a 1D lattice and $\mathbf{c}_{\ell} = (c_{\ell\uparrow}, c_{\ell\downarrow})^T$. $\vec{B} = B \vec{n}_B$ and $\vec{\lambda} = \lambda \vec{n}_{\lambda}$, with $B, \lambda \geq 0$ are the magnetic field and the SOC oriented along the spacial directions \vec{n}_B and \vec{n}_{λ} , respectively. The components of the vector $\vec{\sigma} = (\sigma_x, \sigma_y, \sigma_z)$ are the Pauli matrices and σ_0 is the 2×2 unitary matrix. This model has a topological phase provided that \vec{n}_{λ} has a non-vanishing component perpendicular to the direction \vec{n}_B . The evaluation of topological invariants [54, 55], leads to the following analytical expressions for the boundaries

$$|2|t| - r| < |\mu| < |2|t| + r|, \quad B |\vec{n}_{\lambda} \cdot \vec{n}_B| < |\Delta| < B, \quad (2)$$

with $r = \sqrt{B^2 - \Delta^2}$.

Geometric characterization of the MZMs. The MZMs of the Hamiltonian of Eq. (1) can be written as

$$\eta_{\nu} = \gamma_{\nu}^{\dagger} + \gamma_{\nu}, \quad (3)$$

where $\nu = L, R$ denotes the left and right end of the wires, respectively. We assume that the spin of γ_{ν}^{\dagger} is oriented along the Bloch vector $\vec{n}_{\nu} = (\cos \theta, \sin \varphi, \cos \theta, \cos \varphi, \sin \theta, \sin \varphi)$. The

angles θ_ν and φ_ν in the Bloch sphere, as well as a phase δ_ν — defined $\text{mod}(\pi)$ — are the GBC, which fully characterize the MZM through

$$\gamma_\nu^\dagger = e^{i\delta_\nu} \left[\cos(\theta_\nu/2) c_{\nu\uparrow}^\dagger + e^{i\varphi_\nu} \sin(\theta_\nu/2) c_{\nu\downarrow}^\dagger \right]. \quad (4)$$

Here, $c_{\nu s}^\dagger$ are fermionic creation operators associated to the basis of H_w , acting at the ends of the wire (usually including a few sites). Importantly, not only the angles θ_ν and φ_ν , but also δ_ν depend on the choice of the reference frame. The change in the coordinates of \vec{n}_ν under a rotation of the coordinate system is a routine exercise. The corresponding change of δ_ν leads to a function $\xi_{L,R}(\vec{n}_L, \vec{n}_R)$, — see Eq. (S5) in the SM [56] — which is a vector potential that depends on \vec{n}_ν but not on δ_ν , generated by a twist between the spin directions [57]. The quantity

$$\delta_{L,R} = \delta_L - \delta_R - \xi_{L,R}(\vec{n}_L, \vec{n}_R) \text{ mod}(\pi), \quad (5)$$

is invariant under rotations. Notice that the SU(2) invariance of $\delta_{L,R}$ is expected since it appears in the evaluation of expectation values of observables, in particular, the Josephson current through the closing contact of a ring formed with the wire, which is threaded by a magnetic flux. In addition, the scalar product of the two unit vectors, $\vec{n}_L \cdot \vec{n}_R$, is also an SU(2)-invariant, which defines the relative tilt of the Bloch vectors of the two MZMs.

Symmetry-imposed properties of the MZMs of a wire. We start by noticing that when $\vec{n}_\lambda \cdot \vec{y} = \vec{n}_B \cdot \vec{y} = 0$, the Hamiltonian is invariant under inversion (defined by the transformation $\ell \leftrightarrow N+1-\ell$, for a chain with N sites) and complex conjugation, implying

$$\delta_R = -\delta_L, \quad \theta_R = \theta_L = \theta \quad \varphi_R = -\varphi_L. \quad (6)$$

The Hamiltonian is also invariant under inversion and simultaneous change in the sign of λ . For $\vec{n}_\lambda \cdot \vec{n}_B = 0$ and $\vec{n}_B \parallel \vec{z}$, the latter change of sign can be absorbed in a gauge transformation $\tilde{c}_{\ell\uparrow}^\dagger = ic_{\ell\uparrow}^\dagger$, $\tilde{c}_{\ell\downarrow}^\dagger = -ic_{\ell\downarrow}^\dagger$. Therefore the MZM for $\nu = R$, has the same form as the one for $\nu = L$, replacing the operators $c_{\ell\sigma}^\dagger$ at the left end by the $\tilde{c}_{\ell\sigma}^\dagger$ at the right. Hence, the GBC at the two ends are related as

$$\delta_R = \delta_L \pm \frac{\pi}{2}, \quad \theta_R = \theta_L = \theta, \quad \varphi_R = \varphi_L + \pi. \quad (7)$$

This means that the Bloch vectors of the MZMs have components perpendicular to \vec{n}_B with opposite signs at the two edges, a conclusion that has been previously reached after the explicit calculation of the wave function in particular frames [49, 51]. We conclude that this property does not depend on the choice of the coordinate frame, since the relative tilt of the spin orientations is invariant under rotations. Furthermore, combining with the condition of Eq. (6), we identify an ECF: $\vec{n}_B \parallel \vec{z}$ and $\vec{n}_\lambda \parallel \vec{x}$. In that frame we have

$$\delta_R = -\delta_L = \pm\pi/4, \quad \varphi_R = -\varphi_L = \pm\pi/2, \quad \theta_R = \theta_L = \theta. \quad (8)$$

In order to conclude the full characterization of the MZMs of Eq. (1) in this frame, we still need to define the signs in

Eq. (8) and find the relation between θ_ν and the parameters of the Hamiltonian of Eq. (1). It is not simple to get analytical expressions in general. In what follows we present results for the case of $B \gg \lambda, |\Delta|$, which will lead to the exact values of φ_ν and δ_ν in all the parameter space. In the SM [56], we show that they coincide with the values for these parameters obtained from the calculation of the continuum version of the model in Ref. [1] in the limit of dominant SOC of the topological phase.

Limit of dominant magnetic field. This limit is intuitively related to Kitaev's model. Albeit, it is important to recall that the nature of the MZMs in the present case is quite different. In fact, they are not fully polarized in the direction of the magnetic field, but the spins are tilted in opposite directions at the two edges, as concluded after Eq. (7).

Our aim now is to explicitly calculate the GBC of the two MZMs as functions of the Hamiltonian parameters λ, Δ, B, μ when B dominates, in the ECF. To this end, it is useful to rewrite the Hamiltonian H_w of the wires in the basis that diagonalizes H_0 in Eq. (1). We introduce the unitary transformation in reciprocal space $d_{k+} = u_k c_{k\uparrow} + v_k c_{k\downarrow}$, $d_{k-} = -v_k c_{k\uparrow} + u_k c_{k\downarrow}$, being $u_k, v_k/\text{sgn}(\lambda_k) = \sqrt{(1 \pm B/r_k)/2}$, with $r_k = \sqrt{\lambda_k^2 + B^2}$, and $\lambda_k = 2\lambda \sin k$. This leads to

$$H_w = \sum_{k,s=+,-} \left(\varepsilon_{k,s} d_{k,s}^\dagger d_{k,s} + \Delta_k^T d_{k,s}^\dagger d_{-k,s}^\dagger \right) + \sum_k \Delta_k^S d_{k+}^\dagger d_{-k-}^\dagger + \text{H.c.} \quad (9)$$

being $\varepsilon_{k,s} = \xi_k \mp r_k$ with $\xi_k = -2t \cos k - \mu$. The pairing interaction contains a triplet component with p-wave symmetry $\Delta_k^T = -\lambda_k \Delta / r_k$ — notice that λ_k is an odd function of k — and a singlet one, $\Delta_k^S = B\Delta / r_k$.

For $B \gg \Delta \gg \lambda$, the transformed model can be solved analytically with the method of Alase *et al.* [2–5] (see SM [56], for details). For $t, \Delta > 0$, and $\mu = -B, \Delta$, the results are

$$\delta_L = -\delta_R = \frac{\pi}{4}, \quad \varphi_L = -\varphi_R = -\frac{\pi}{2}, \quad (10)$$

$$\theta \sim \frac{\Delta}{B + \sqrt{(B^2 - t^2)}} + O\left(\frac{\lambda}{B}\right), \quad \vec{n}_B = \vec{z}, \quad \vec{n}_\lambda = \vec{x}.$$

While Eq. (8) gives the values of δ_ν and φ_ν up to a sign, Eq. (10) gives their exact values. Although the calculation was done for dominant magnetic field, this result should be valid for continuity in all the topological phase with $B, t, \Delta, \lambda > 0, \mu < 0$. The corresponding values for the opposite signs and orientations of these parameters can be deduced by means of symmetry arguments [62].

It is important to highlight that the previous results and appropriate SU(2) rotations permit to obtain exactly δ_ν and φ_ν in any coordinate system for any value of the parameters of Eq. (1) with $\vec{n}_\lambda \cdot \vec{n}_B = 0$, while θ needs an explicit calculation. Our goal now is to show that this angle can be inferred from the behavior of the Josephson current in suitably designed junctions.

Josephson current. In order to calculate the Josephson current we consider two wires w1 and w2 with different phases ϕ_1, ϕ_2 of the pairing potentials, related as $\phi_1 - \phi_2 = \phi$ and connected

by a tunneling term, as indicated in the sketches of Figs. 2 and 3. Gauging out the dependence on ϕ in the operators of the wires, the Hamiltonian for the full system reads $H(\phi) = H_{w1} + H_{w2} + H_c(\phi)$, where H_{w1} , H_{w2} have the same structure as in Eq. (1). The connecting term reads

$$H_c(\phi) = t_c \sum_{\sigma=\uparrow,\downarrow} \left(e^{i\phi/2} c_{1,\sigma}^\dagger c_{2,\sigma} + \text{H.c.} \right), \quad (11)$$

with 1 and 2 denoting, respectively, the site at the right/left end of w1/w2. We can calculate the current numerically as described in the SM [56]. In the topological phase, however, a simple description based on the coupling of the MZMs accurately explains the Andreev spectrum and the Josephson current. This is because, in a topological junction, Andreev states are formed from the hybridization of the MZMs [19, 41, 45].

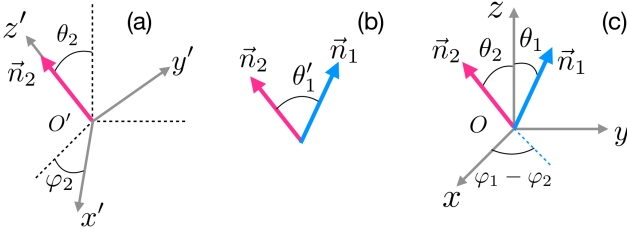


FIG. 1. (a) Reference frame with \vec{z}' along the Bloch vector of the MZM of w2. (b) Bloch vector of the MZMs of the two wires. (c) Reference frame of H_{w_j} , $j = 1, 2$ (laboratory frame).

In what follows we derive the low-energy effective Hamiltonian H_{eff} that describes the hybridization of the MZMs. Importantly, we consider different magnetic fields and SOC orientations in the two wires. H_{eff} takes a particularly simple form if the quantization axis is chosen in the direction of the Bloch vector of one of the MZMs next to the junction, which we choose to be \vec{n}_2 . In the basis where $\vec{n}_2 \equiv \vec{z}'$ — see Fig. 1 (a) — the spin down operators of the sites nearest to the junction contribute only at high energies, while the low-energy component is precisely the contribution of the MZM. Concretely, we can substitute the fermionic operators at the ends of the wires by their projection on the MZMs,

$$c'_{1\uparrow} \simeq \frac{a_1}{2} e^{i\delta'_1} \cos\left(\frac{\theta'_1}{2}\right) \eta_1, \quad c'_{2\uparrow} \simeq \frac{a_2}{2} e^{i\delta'_2} \eta_2, \quad (12)$$

where θ'_1 is the angle between \vec{n}_1 and \vec{n}_2 — see Fig. 1 (b) — and δ'_1, δ'_2 are the corresponding phases. a_i are real numbers, $a_i^2 \leq 1$ being the weight of the MZMs on the corresponding site at the boundary of each chain. Replacing in Eq. (S47) we obtain

$$H_{\text{eff}}(\phi) = \frac{t_J(\theta'_1)}{2} \sin\left(\frac{\phi}{2} + \delta'_2 - \delta'_1\right) i\eta_1 \eta_2, \quad (13)$$

$$t_J(\theta'_1) = t_c a_1 a_2 \cos\left(\frac{\theta'_1}{2}\right), \quad (14)$$

which is solved by defining a fermion $d = (\eta_1 + i\eta_2)/2$ [4], leading to $i\eta_1 \eta_2 = 2d^\dagger d - 1$. The ground-state energy is

$$E_{\text{eff}}(\phi) = -\frac{1}{2} |t_J(\theta'_1)| \left| \sin\left(\frac{\phi'}{2}\right) \right|, \quad (15)$$

where $\phi' = \phi + 2(\delta'_2 - \delta'_1)$. The Josephson current is

$$J_{\text{eff}}(\phi) = \frac{2e}{\hbar} \frac{dE_{\text{eff}}(\phi)}{d\phi} = -\frac{e|t_J(\theta'_1)|}{2\hbar} \cos\left(\frac{\phi'}{2}\right) \text{sgn}\left\{\sin\left(\frac{\phi'}{2}\right)\right\}. \quad (16)$$

Performing the rotation sketched in Fig. 1 (see SM [56] for details), we can express this current in terms of the GBC of the MZMs of w1 and w2 next to the junction in the laboratory frame through

$$\phi' = \phi + 2(\delta_2 - \delta_1 - \xi_{1,2}), \quad (17)$$

where δ_1 and δ_2 are the corresponding phases and

$$\xi_{1,2} = \arctan\left[\frac{\sin(\varphi_1 - \varphi_2)}{\cos(\varphi_1 - \varphi_2) + \cot\left(\frac{\theta_1}{2}\right) \cot\left(\frac{\theta_2}{2}\right)} \right]. \quad (18)$$

The different angles are indicated in Fig. 1. We would like to stress that all the quantities that determine the behavior of the Josephson current are SU(2)-invariant, as explicitly shown in Ref. [56]. In particular, θ'_1 does not depend on the reference frame while $\delta_2 - \delta_1 - \xi_{1,2}$ is an invariant akin to Eq. (5) and from Eq. (17) we clearly see that this quantity plays the role of a geometric phase that modifies the magnetic flux.

The Josephson current of Eq. (16) has a jump at $\phi' = 0$ as a consequence of the crossing of levels with different fermion parity. If parity is conserved, the typical 4π -periodicity of topological junctions is obtained. In the case of junctions of wires with the same orientation of the magnetic field and SOC, $\delta_1 - \delta_2 = \pm\pi$, as given by Eq. (7), and the jump occurs at $\phi = \pi$. However, in junctions of wires having different orientations of \vec{n}_B and \vec{n}_λ , this may take place at other values of ϕ . In what follows, we analyze junctions of wires with different configurations of these vectors with the aim of using the behavior of the Josephson current to extract information of the MZMs.

Junctions with tilt in the SOC. We consider the same orientation of the magnetic field in both wires, but a tilt β_λ in the orientation the SOC, i.e. $\vec{n}_{\lambda,1} \cdot \vec{n}_{\lambda,2} = \cos\beta_\lambda$. This can be realized with a junction where the wires are placed on the superconducting substrate forming an angle β_λ , as in the sketch of Fig. 2, where we also indicate the ECF for w2 ($\vec{n}_B \parallel \vec{z}$ and $\vec{n}_{\lambda,2} \parallel \vec{x}$). We focus on $\Delta > 0$, $\mu < 0$, in which case Eqs. (10) give δ_2 and φ_2 , while δ_1 and φ_1 can be also derived from these Eqs. by performing a rotation of β_λ around \vec{z} . This leads to $\theta_1 = \theta_2 = \theta$, $\varphi_1 - \varphi_2 = \pi - \beta_\lambda$ and $\delta_1 = \delta_2 + (\pi + \beta_\lambda)/2$. Replacing in Eqs. (17) and (S5) we obtain

$$\phi' = \phi - \pi - \beta_\lambda + 2 \arctan\left[\frac{\sin(\beta_\lambda)}{\cos(\beta_\lambda) - \cot^2\left(\frac{\theta}{2}\right)} \right]. \quad (19)$$

Therefore, from the position of the jump in the current as a function of the flux it is possible to extract the angle θ between the Bloch vector of the MZMs with respect to \vec{n}_B . This

completes the full description of the MZMs at both sides of the junction. In Fig. 2, we show results calculated with H_{eff} , and by exact diagonalization of the full Hamiltonian $H(\phi)$ (see Ref [56] for technical details). Both calculations are in excellent agreement and also agree with results reported in the limit of weak SOC in the continuum model [63] and in the limit of large B [64].

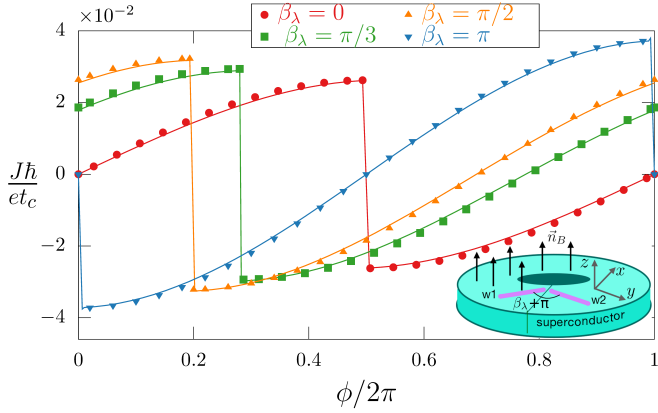


FIG. 2. Josephson current as a function of the flux for several values of the angle β_λ between the orientation of the SOC in the two wires, keeping $\vec{n}_B \cdot \vec{n}_\lambda = 0$ in both wires. Solid lines: numerical results. Symbols: J_{eff} calculated using H_{eff} . Parameters are $t = 1$, $B = 4$, $\lambda = 2$, $\Delta = 2$ and $\mu = -3$.

Junctions with tilt in the magnetic field. We now focus on the case where the SOC is equally oriented in the two wires, $\vec{n}_{\lambda,1} = \vec{n}_{\lambda,2} = \vec{x}$, while the orientation of the magnetic field $\vec{n}_{B,1}$ is tilted by an angle β_B with respect to $\vec{n}_{B,2} \parallel \vec{z}$. We start with the case $\vec{n}_{\lambda,j} \cdot \vec{n}_{B,j} = 0$, $j = 1, 2$, which can be realized in the two configurations sketched in Fig. 3. As before, for $\Delta > 0$, $\mu < 0$, Eqs. (10) give us the values of δ_2 and φ_2 . On the other hand, the corresponding values of δ_1 and φ_1 can also be obtained from these Eqs. by performing a rotation of angle β_B around \vec{x} . These are $\delta_1 = -\pi/4$ and $\varphi_1 = (\pi/2)\text{sgn}[\sin(\theta_2 - \beta_B)]$ and $\theta_1 = \theta_2 - \beta_B$. Hence, the Josephson current is given by Eq. (16) with $\phi' = \phi - \pi$. Therefore, the *shape* of the function $J(\phi)$ is the same for all values of β_B , displaying a jump at $\phi = \pi$. However, the *magnitude* of the current depends on the angles θ_2 and β_B according to Eq. (14), with $\theta'_1 = 2\theta_2 - \beta_B$. This is illustrated in Fig. 3 and has a simple interpretation. For $\beta_B = 0$, \vec{n}_1 and \vec{n}_2 have the same z component, $\theta_1 = \theta_2$, zero x component and opposite y components [see Eqs. (7) and (10)]. Rotating $\vec{n}_{B,1}$ around the x axis, \vec{n}_1 is moved towards \vec{n}_2 and both vectors coincide when $\beta_B = 2\theta_2$. This angle corresponds to the maximum of $t_j(\theta'_1)$, hence, the maximum of $J(\phi)$ at fixed ϕ . In addition, for fixed fermion parity, the Josephson current is 4π -periodic in β_B , in agreement with Ref. 20. When the magnetic field is tilted in such a way that there is a finite component along the direction of the SOC there is no simple analytical expression relating the tilt in the magnetic field and the orientation of the Bloch vector of the MZMs and we must rely on the full expressions given by Eqs. (16), (17)

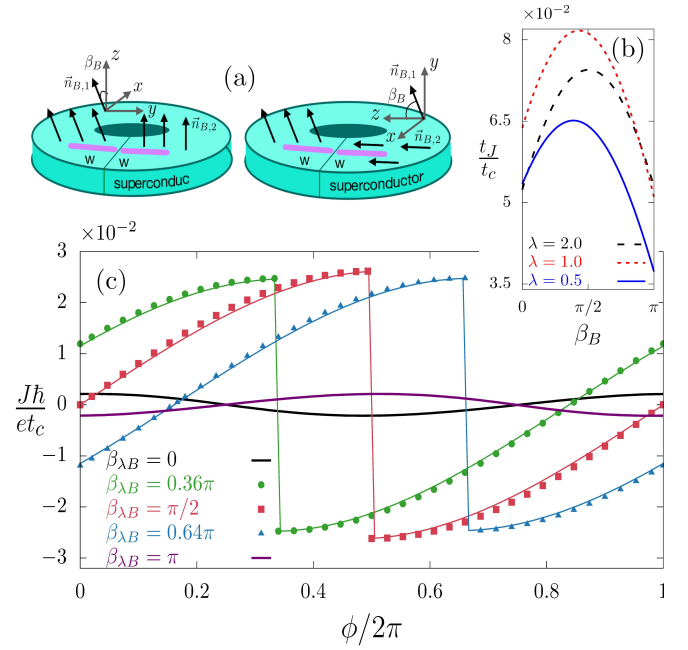


FIG. 3. (a) Configurations of wires corresponding to wires with a tilt β_B in the orientation of the magnetic field with $\vec{n}_B \cdot \vec{n}_\lambda = 0$. (b) Amplitude of the Josephson current t_J as a function of β_B for $\vec{n}_B \cdot \vec{n}_\lambda = 0$. (c) Josephson current as a function of ϕ for $\vec{n}_{\lambda,1} = \vec{n}_{\lambda,2}$, $\vec{n}_{B,2} \cdot \vec{n}_{\lambda,2} = 0$, $\vec{n}_{B,1} \cdot \vec{n}_{\lambda,1} = \cos \beta_{\lambda B}$ and all vectors in the same plane. Solid lines: numerical results. Symbols: J_{eff} calculated using H_{eff} . Parameters are $t = 1$, $B = 4$, $\lambda = 2$, $\Delta = 2$ and $\mu = -3$.

and (S5). In Fig. 3 (c) we show the Josephson current $J(\phi)$ for the case in which $\vec{n}_{\lambda,1} = \vec{n}_{\lambda,2}$, $\vec{n}_{B,2} \cdot \vec{n}_{\lambda,2} = 0$ and $\vec{n}_{B,1}$ is tilted keeping it perpendicular to $\vec{n}_{B,2} \wedge \vec{n}_{\lambda,2}$, and forming an angle $\beta_{\lambda B}$ with $\vec{n}_{\lambda,i}$. Without tilting $J(\phi) = 0$ as expected [65]. For other cases, $J(\phi)$ presents jumps at $\phi \neq \pi$ as in the case of wires with SOC perpendicular to B but with a relative tilt, analyzed in Fig. 2. It is found again an excellent agreement between the description in terms of the effective Hamiltonian $H_{\text{eff}}(\phi)$ and the numerical solution of the exact Hamiltonian (see Ref. [56] for details). For small $\beta_{\lambda B}$, the topological phase is lost in w1 leaving its place to a non-topological phase — see of Eq. (2) — which is gapless for a wide parameter range. There, $H_{\text{eff}}(\phi)$ is no longer useful and the numerical solution of $H(\phi)$ is necessary, which leads to a smooth behavior of $J(\phi)$, typical of ordinary superconductors with small amplitude, albeit preserving some peculiar features of the topological phase, like a non-vanishing current for $\phi = 0$ [65], similar to Ref. [66].

Conclusions. We have characterized the MZMs of topological superconducting wires with SOC and magnetic field in terms of GBC $(\varphi, \theta, \delta)$. We have analytically calculated φ, δ for the ECF where $\vec{n}_B \equiv \vec{z}$ and $\vec{n}_\lambda \equiv \vec{x}$. We have also derived the transformation of these quantities under changes of the reference frame. We used these results to derive exact expressions for the Josephson current in wires having relative

tilts in the orientations of the SOC and magnetic fields. We showed that for suitable configurations of the junctions, the dc Josephson current provides the necessary information to fully reconstruct the structure of the MZMs. These results may be useful in the experimental implementation of quantum tomography of MZMs through the information provided by the dc Josephson current. The dc regime could be reached, for instance, by adiabatically switching on the magnetic field or by rotating it from the gapless non-topological phase of nearly parallel spin-orbit coupling and magnetic field. This is possible within the present experimental state of the art of the hybrid superconducting-semiconducting wires we have studied [12]. Interestingly, this regime is free from the problem of the time-scales introduced by the poor equilibration of the MZMs which affect readout processes of dynamical effects [67–69].

Acknowledgments. LA thanks A. Levy Yeyati and F. von Oppen for stimulating discussions. We acknowledge support from CONICET, Argentina and the Alexander von Humboldt Foundation, Germany (LA). We are sponsored by PIP-RD 20141216-4905 and PIP 112-201501-00506 of CONICET, PICT-2017-2726, PICT-2018-04536 and PICT-Raices-2018.

-
- [1] A. Y. Kitaev, *Sov. Phys. Usp.* **44**, 131 (2001).
 [2] J. Alicea, *Rep. Prog. Phys.* **75**, 076501, (2012).
 [3] M. H. Freedman, M. Larsen, Z. Wang, *Commun. Math. Phys.* **227**, 605 (2002).
 [4] A. Kitaev, *Ann. Phys. (N.Y.)* **303**, 2 (2003).
 [5] Y. Oreg, G. Refael, and F. von Oppen, *Phys. Rev. Lett.* **105**, 177002 (2010).
 [6] R. M. Lutchyn, J. Sau, and S. Das Sarma, *Phys. Rev. Lett.* **105**, 077001 (2010).
 [7] V. Mourik, K. Zuo, S. M. Frolov, S. R. Plissard, E. P. a. M. Bakkers, and L. P. Kouwenhoven, *Science* **336**, 1003 (2012).
 [8] L. P. Rokhinson, X. Liu and J. K. Furdyna, *Nat. Phys.* **8**, 795 (2012).
 [9] A. Das, Y. Ronen, Y. Most, Y. Oreg, M. Heiblum, and H. Shtrikman, *Nat. Phys.* **8**, 887 (2012).
 [10] S. M. Albrecht, A. P. Higginbotham, M. Madsen, F. Kuemmeth, T. S. Jespersen, J. Nyg, P. Krogstrup, and C. M. Marcus, *Nature* **531**, 206 (2016).
 [11] M. Deng, S. Vaitiekenas, E. Hansen, J. Danon, M. Leijnse, K. Flensberg, J. Nygård, P. Krogstrup, and C. Marcus, *Science* **354**, 1557 (2016).
 [12] D. Razmadze, E. C. T. O’Farrell, P. Krogstrup and C. M. Marcus, *arXiv:2005.11848*.
 [13] H. Kwon, K. Sengupta, and V. Yakovenko, *Eur. Phys. J. B* **37**, 349 (2004).
 [14] L. Fu and C. L. Kane, *Phys. Rev. B* **79**, 161408 (2009).
 [15] D. M. Badiane, M. Houzet, and J. S. Meyer, *Phys. Rev. Lett.* **107**, 177002 (2011).
 [16] L. Jiang, D. Pekker, J. Alicea, G. Refael, Y. Oreg, F. von Oppen, *Phys. Rev. Lett.* **107**, 236401 (2011).
 [17] C. W. J. Beenakker, D. I. Pikulin, T. Hyart, H. Schomerus, and J. P. Dahlhaus, *Phys. Rev. Lett.* **110**, 017003 (2013).
 [18] A. Zazunov and R. Egger, *Phys. Rev. B* **85**, 104514 (2012).
 [19] F. Pientka, A. Romito, M. Duckheim, Y. Oreg, F. von Oppen, *New J. Phys.* **15**, 025001 (2013).
 [20] F. Pientka, L. Jiang, D. Pekker, J. Alicea, G. Refael, Y. Oreg, F. von Oppen *New J. Phys.* **15**, 115001 (2013).
 [21] P. Marra, R. Citro, A. Braggio, *Phys. Rev. B* **93**, 220507(R) (2016).
 [22] Y. Peng, F. Pientka, E. Berg, Y. Oreg, and F. von Oppen, *Phys. Rev. B* **94**, 085409 (2016).
 [23] J. I. Väyrynen, G. Rastelli, W. Belzig, and L. I. Glazman, *Phys. Rev. B* **92**, 134508 (2015).
 [24] M. Trif, O. Dmytruk, H. Bouchiat, R. Aguado, and P. Simon, *Phys. Rev. B* **97**, 041415 (2018).
 [25] J. Cayao, E. Prada, P. San-José, and R. Aguado, *Phys. Rev. B* **91**, 024514 (2015).
 [26] A. Zazunov, R. Egger, and A. Levy Yeyati, *Phys. Rev. B* **94**, 014502 (2016).
 [27] E. B. Hansen, J. Danon, and K. Flensberg, *Phys. Rev. B* **93**, 094501 (2016).
 [28] J. Cayao, A. M. Black-Schaffer, E. Prada, and R. Aguado, *Beilstein J. Nanotechnol.* **9**, 1339 (2018).
 [29] A. Zazunov, A. Iks, M. Alvarado, A. Levy Yeyati, and R. Egger, *Beilstein J. Nanotechnol.* **9**, 1659 (2018).
 [30] A. Schuray, A. Levy Yeyati, and P. Recher, *Phys. Rev. B* **98**, 235301 (2018).
 [31] P. San-Jose, E. Prada, and R. Aguado, *Phys. Rev. Lett.* **108**, 257001 (2012).
 [32] D. I. Pikulin and Y. V. Nazarov, *Phys. Rev. B* **86**, 140504(R) (2012).
 [33] S.-P. Lee, K. Michaeli, J. Alicea, and A. Yacoby, *Phys. Rev. Lett.* **113**, 197001 (2014).
 [34] D. M. Badiane, L. I. Glazman, M. Houzet, and J. S. Meyer, *Comptes Rendus Physique* **14**, 840 (2013).
 [35] Y. Peng, Y. Vinkler-Aviv, P. W. Brouwer, L. I. Glazman, and F. von Oppen, *Phys. Rev. Lett.* **117**, 267001 (2016).
 [36] D. Sticlet, J. D. Sau, and A. Akhmerov, *Phys. Rev. B* **98**, 125124 (2018).
 [37] S. B. Chung, J. Horowitz, and X.-L. Qi, *Phys. Rev. B* **88**, 214514 (2013).
 [38] A. Keselman, L. Fu, A. Stern, E. Berg, *Phys. Rev. Lett.* **111**, 116402 (2013).
 [39] E. Mellars and B. Béri, *Phys. Rev. B* **94**, 174508 (2016).
 [40] X.-J. Liu, C. L. M. Wong, and K. T. Law, *Phys. Rev. X* **4**, 021018 (2014).
 [41] A. Camjayi, L. Arrachea, A. Aligia and F. von Oppen, *Phys. Rev. Lett.* **119**, 046801 (2017).
 [42] C. Schrade and L. Fu, Parity-controlled 2π Josephson effect mediated by Majorana Kramers pairs, *Phys. Rev. Lett.* **120**, 267002 (2018).
 [43] L. Lauke, M. S. Scheurer, A. Poenicke, and J. Schmalian, *Phys. Rev. B* **98**, 134502 (2018).
 [44] A. Haim and Y. Oreg, *Phys. Rep.* **825**, 1 (2019).
 [45] L. Arrachea, A. Camjayi, A. A. Aligia, and L. Gruñeiro, *Phys. Rev. B* **99**, 085431 (2019).
 [46] Arbel Haim, *Phys. Rev. B* **100**, 064505 (2019).
 [47] M. Alvarado, A. Iks, A. Zazunov, R. Egger, A. Levy Yeyati, *Phys. Rev. B* **101**, 094511 (2020).
 [48] C. Knapp, A. Chew, and J. Alicea, *arXiv:2006.10772*.
 [49] D. Sticlet, C. Bena, and P. Simon, *Phys. Rev. Lett.* **108**, 096802 (2012).
 [50] M. Serina, D. Loss, and J. Klinovaja, *Phys. Rev. B* **98**, 035419 (2018).
 [51] E. Prada, R. Aguado, P. San-Jose, *Phys. Rev. B* **96**, 085418 (2017).
 [52] J. Osca, D. Ruiz, and L. Serra, *Phys. Rev. B* **89**, 245405 (2014).
 [53] S. Rex and A. Sudbo, *Phys. Rev. B* **90**, 115429 (2014).

- [54] S. Tewari and J. D. Sau, Phys. Rev. Lett. **109**, 150408 (2012).
 [55] J. C. Budich and E. Ardonne, Phys. Rev. B **88**, 075419 (2013).
 [56] See Supplementary Material for the transformation properties of different quantities under SU(2) rotations, the values of δ , θ and ϕ for certain parameters, and details about the numerical calculations.
 [57] K. Hamamoto, M. Ezawa, and N. Nagaosa, Phys. Rev. B **92**, 115417 (2015).
 [58] A. Alase, E. Cobanera, G. Ortiz, and L. Viola, Phys. Rev. Lett. **117**, 076804 (2016).
 [59] A. Alase, E. Cobanera, G. Ortiz, and L. Viola, Phys. Rev. B **96**, 195133 (2017).
 [60] A. A. Aligia and L. Arrachea, Phys. Rev. B **98**, 174507 (2018).
 [61] A. A. Aligia and A. Camjayi, Phys. Rev. B **100**, 115413 (2019).
 [62] A change of sign of Δ can be absorbed by a gauge transformation $\tilde{c}_{j\sigma}^\dagger \rightarrow ic_{j\sigma}^\dagger$ that has the effect of flipping the sign of δ in Eqs. (10). A change of sign of $\lambda(t)$ for $\vec{n}_\lambda \cdot \vec{y} = 0$ can be compensated taking the complex conjugate of H (complex conjugation and $c_{j\sigma} \rightarrow (-1)^j c_{j\sigma}$) and its effect is to change the sign of both δ and φ . Using time reversal, a change in sign of B has the effect on Eq. (10) of replacing θ by $\pi - \theta$ and inverting the sign of φ . Charge conjugation $c_{j\sigma}^\dagger \rightarrow c_{j\sigma}$ and complex conjugation, which leaves the Majorana invariant, changes the sign of all parameters. By consistency a change in sign of μ has the effect of replacing θ by $\pi - \theta$.
 [63] J. Klinovaja and D. Loss. Eur. Phys. J. B **88**, 62 (2015).
 [64] Christian Spänslätt, Phys. Rev. B **98**, 054508 (2018).
 [65] Notice that necessary conditions for a non-vanishing current are breaking of the time-reversal and the spacial inversion symmetry introduced below Eq. (6).
 [66] A. Zazunov, R. Egger, T. Jonckheere, and T. Martin, Phys. Rev. Lett. **103**, 147004 (2009).
 [67] N. Bondyopadhaya and D. Roy, Phys. Rev. B **99**, 214514 (2019).
 [68] R. Seoane Souto, K. Flensburg, and M. Leijnse, Phys. Rev. B **101**, 081407(R) (2020).
 [69] R. Tuovinen, E. Perfetto, R. van Leeuwen, G. Stefanucci, and M. A. Sentef, New. J. Phys. **21**, 103038 (2019).

Supplemental Material: Tomography of zero-energy end modes in topological superconducting wires

CHANGE OF REFERENCE FRAME

General case

The spin of the fermionic creation operators defined in Eq. (4) of the main text is expressed in a given reference frame O , determined by the quantization axis of the Hamiltonian H_w . Here, we analyze the transformation of the spin under a change of basis to a rotated frame O' . We remind the reader that under an active transformation, (a rotation of the physical system an angle α around de unit vector \vec{v} keeping the coordinates unchanged) a state $|\psi\rangle = (ac_\uparrow^\dagger + bc_\downarrow^\dagger)|0\rangle$, becomes $R_{\vec{v}}(\alpha)|\psi\rangle$, where the SU(2) matrix $R_{\vec{v}}(\alpha)$ is

$$R_{\vec{v}}(\alpha) = \cos\left(\frac{\alpha}{2}\right) - i \sin\left(\frac{\alpha}{2}\right) \vec{v} \cdot \vec{\sigma}. \quad (S1)$$

If, instead, the physical system is fixed and the rotation is applied to the coordinate system O to transform it to O' , the state in the new basis is $|\psi'\rangle = R_{\vec{v}}^{-1}(\alpha)|\psi\rangle$. Inverting the previous transformation we obtain for the creation operators

$$\begin{aligned} c_\uparrow^\dagger &= \left(\cos\left(\frac{\alpha}{2}\right) + e^{-i\frac{\alpha}{2}} v_z \right) (c'_\uparrow)^\dagger + \sin\left(\frac{\alpha}{2}\right) (v_y - iv_x) (c'_\downarrow)^\dagger \\ c_\downarrow^\dagger &= -\sin\left(\frac{\alpha}{2}\right) (v_y + iv_x) (c'_\uparrow)^\dagger + \left(\cos\left(\frac{\alpha}{2}\right) + v_z e^{i\frac{\alpha}{2}} \right) (c'_\downarrow)^\dagger, \end{aligned} \quad (S2)$$

where v_j is the component of \vec{v} in the direction j . Replacing this transformation in Eq. (4) of the main text we obtain the expression of the creation component of the MZM in the rotated frame O' :

$$\begin{aligned} \gamma_v^\dagger &= e^{i\delta_v} \left[A(c'_\uparrow)^\dagger + B(c'_\downarrow)^\dagger \right], \\ A &= \cos\left(\frac{\theta_v}{2}\right) \left(\cos\left(\frac{\alpha}{2}\right) + e^{-i\frac{\alpha}{2}} v_z \right) - e^{i\varphi_v} \sin\left(\frac{\theta_v}{2}\right) \sin\left(\frac{\alpha}{2}\right) (v_y + iv_x), \\ B &= \cos\left(\frac{\theta_v}{2}\right) \sin\left(\frac{\alpha}{2}\right) (v_y - iv_x) + e^{i\varphi_v} \sin\left(\frac{\theta_v}{2}\right) \left(\cos\left(\frac{\alpha}{2}\right) + v_z e^{i\frac{\alpha}{2}} \right). \end{aligned} \quad (S3)$$

Expressing γ_v^\dagger in the same form as Eq. (4) of the main text we get

$$\gamma_v^\dagger = e^{i\delta'_v} \left[\cos\left(\frac{\theta'_v}{2}\right) (c'_{v\uparrow})^\dagger + e^{i\varphi'_v} \sin\left(\frac{\theta'_v}{2}\right) (c'_{v\downarrow})^\dagger \right], \quad (S4)$$

from where the parameters in the frame O' can be obtained. Writing $A = |A|e^{i\xi_v}$, it is clear that $\delta'_v = \xi_v + \delta_v$ being

$$\xi_v = \arctan\left(\frac{\text{Im}A}{\text{Re}A}\right) = \arctan\left(\frac{-\cos(\frac{\theta_v}{2})\sin(\frac{\alpha}{2})v_z - \sin(\varphi_v)\sin(\frac{\theta_v}{2})\sin(\frac{\alpha}{2})v_y - \cos(\varphi_v)\sin(\frac{\theta_v}{2})\sin(\frac{\alpha}{2})v_x}{\cos(\frac{\theta_v}{2})\cos(\frac{\alpha}{2})(1+v_z) - \cos(\varphi_v)\sin(\frac{\theta_v}{2})\sin(\frac{\alpha}{2})v_y + \sin(\varphi_v)\sin(\frac{\theta_v}{2})\sin(\frac{\alpha}{2})v_x}\right). \quad (\text{S5})$$

We see that in general, the phases δ_v transform in a non trivial way under rotations or a change in coordinates. Instead, as expected, the directions \vec{n}_v (defined by θ_v and φ_v) transform as ordinary vectors. Comparing Eqs. (S3) and (S4) we see that $B/A = |B/A|e^{i\varphi'_v}$ or $\bar{A}B = |\bar{A}B|e^{i\varphi'_v}$ (\bar{A} denotes the complex conjugate of A), and $|A| = \cos(\theta'_v/2)$, from which θ_v and φ_v are easily obtained:

$$\theta'_v = 2 \arccos(|A|) = 2 \arctan(|B/A|). \quad (\text{S6})$$

$$\varphi'_v = \arctan\left(\frac{\text{Im}(\bar{A}B)}{\text{Re}(\bar{A}B)}\right), \quad (\text{S7})$$

Derivation of Eq. (18)

In the main text, we evaluate the Josephson current through the connection between wires w1 and w2, with the parameters defined with respect to a frame O' with $\vec{n}_2 \parallel \vec{z}'$, being \vec{n}_2 the direction of the polarization of the MZM of the wire w2 that hybridizes with the MZM of the wire w1 in the junction. The consequent expression for the Josephson current –see Eq. (16) of the main text– depends on the Josephson phase ϕ , as well as on the phases δ'_1 and δ'_2 of the two hybridized MZMs, which depend on the reference frame. Since we know the values of these phases, given the values of the parameters of the Hamiltonians for the wires only when the latter are written in the reference frame O where $\vec{n}_B \parallel \vec{z}$ and $\vec{n}_A \parallel \vec{x}$ –see Eq. (10)– we need to implement a transformation between O' and O . The concrete transformation is sketched in Fig. 1 of the main text. In the formalism described above, this corresponds to a rotation $R_{\vec{v}}(\alpha)$ that transforms O to O' such that $R_{\vec{v}}(\alpha)\vec{n}_2 = \vec{z}$. We choose \vec{v} in the direction of $\vec{n}_2 \wedge \vec{z}$, so that it is perpendicular to both \vec{n}_2 and \vec{z} , hence a positive rotation in the angle $\alpha = \theta_2$ moves \vec{n}_2 to \vec{z} . The components of the unit vector \vec{v} become $v_x = \sin(\varphi_2)$, $v_y = -\cos(\varphi_2)$, $v_z = 0$.

Replacing these values in Eq. (S5) for $v = 2$, we see that the numerator vanishes, and therefore $\xi_2 = 0$, $\delta'_2 = \delta_2$. Instead for $v = 1$ we obtain $\delta'_1 = \xi_1 + \delta_1$, with

$$\xi_1 = \arctan\left(\frac{\sin(\varphi_1 - \varphi_2)}{\cot(\frac{\theta_1}{2})\cot(\frac{\theta_2}{2}) + \cos(\varphi_1 - \varphi_2)}\right). \quad (\text{S8})$$

Combining the $\delta'_2 - \delta'_1$, we get Eqs. (17) and (18) of the main text, with $\xi_{1,2} \equiv \xi_1$, given above.

SU(2) invariance of d_{12}

In this section we prove the SU(2) invariance of the quantity

$$d_{12} = \delta_1 - \delta_2 - \xi_{1,2}, \quad \xi_{1,2} = \arctan\left(\frac{\sin(\varphi_1 - \varphi_2)}{\cot(\frac{\theta_1}{2})\cot(\frac{\theta_2}{2}) + \cos(\varphi_1 - \varphi_2)}\right), \quad (\text{S9})$$

mod(π) for any two fermions of the form of Eq. (4) of the main text [same as Eq. (S4) without the superscript prime]. The fact that the quantity is defined mod(π) means that the branch and discontinuities of the arctan are unimportant. The invariance of d_{12} is expected, since in the particular case discussed in Section , it enters the equation of the Josephson current through ϕ' [see Eqs. (17) of the main text] and the current is an observable. Here, we prove it explicitly for the general case.

As is well known, any SU(2) rotation can be obtained by composing infinitesimal rotations around three mutually perpendicular axis and the generators of these rotations ($i\sigma_x$, $i\sigma_y$ and $i\sigma_z$ in Section) form a basis of the Lie algebra of the group. Two generators are enough for our purposes because the third one is the commutator of the other two times a factor. The invariance of d_{12} under any rotation around z immediately verified since θ_1 and θ_2 , as well as $\delta_1 - \delta_2$ and $\varphi_1 - \varphi_2$ are unchanged under this transformation. Therefore, it remains to prove that d_{12} is invariant under a rotation through an axis perpendicular to z . We choose the y axis in a reference frame with $\varphi_2 = 0$ to simplify the calculation (the axis forming an angle $\pi/2 + \varphi_2$ with the x axis in the original reference frame).

We use the results of Section for $\vec{v} = \vec{y}$, $\varphi_2 = 0$ and $\alpha \rightarrow 0$ to linear order in the differential $d\alpha$ of the angle of the rotation. In particular we replace $\cos(\alpha/2) \simeq 1$ and $\sin(\alpha/2) \simeq d\alpha/2$. From Eq. (S5) we obtain the change in the phase under the infinitesimal rotation, $d\delta_\nu = \delta'_\nu - \delta_\nu$,

$$d\delta_\nu = d \arctan(\delta_\nu) = -\frac{\frac{d\alpha}{2} \sin(\varphi_\nu) \sin(\frac{\theta_\nu}{2})}{\cos(\frac{\theta_\nu}{2})}. \quad (\text{S10})$$

Evaluating explicitly for $\nu = 1, 2$ this equation reads

$$\frac{d\delta_1}{d\alpha} = -\frac{1}{2} \tan\left(\frac{\theta_1}{2}\right) \sin(\varphi_1), \quad \frac{d\delta_2}{d\alpha} = 0. \quad (\text{S11})$$

From Eqs. (S3) and (S6) we get

$$\cot\left(\frac{\theta'_\nu}{2}\right)^2 = \cot\left(\frac{\theta_\nu}{2}\right)^2 \frac{1 - \tan(\frac{\theta_\nu}{2}) \cos(\varphi_\nu) d\alpha}{1 + \cot(\frac{\theta_\nu}{2}) \cos(\varphi_\nu) d\alpha} = \cot\left(\frac{\theta_\nu}{2}\right)^2 \left(1 - \cos(\varphi_\nu) d\alpha \left(\tan\left(\frac{\theta_\nu}{2}\right) + \cot\left(\frac{\theta_\nu}{2}\right)\right)\right) \quad (\text{S12})$$

$$d \cot\left(\frac{\theta_\nu}{2}\right)^2 = -\cot\left(\frac{\theta_\nu}{2}\right)^2 \left(\tan\left(\frac{\theta_\nu}{2}\right) + \cot\left(\frac{\theta_\nu}{2}\right)\right) \cos(\varphi_\nu) d\alpha. \quad (\text{S13})$$

Using that for any function r , $dr^2 = 2rdr$ we obtain

$$\frac{d \cot(\theta_1/2)}{d\alpha} = -\frac{\cos(\varphi_1)}{2} \left(1 + \cot\left(\frac{\theta_1}{2}\right)^2\right) \quad (\text{S14})$$

$$\frac{d \cot(\theta_2/2)}{d\alpha} = -\frac{1}{2} \left(1 + \cot\left(\frac{\theta_2}{2}\right)^2\right) \quad (\text{S15})$$

The change of the angles $d\varphi_\nu = \varphi'_\nu - \varphi_\nu$ are obtained using Eqs. (S3) and (S7)

$$\tan(\varphi'_\nu) = \frac{\sin(\varphi_\nu) \sin(\frac{\theta_\nu}{2}) \cos(\frac{\theta_\nu}{2})}{\cos(\varphi_\nu) \sin(\frac{\theta_\nu}{2}) \cos(\frac{\theta_\nu}{2}) + (\cos(\frac{\theta_\nu}{2})^2 - \sin(\frac{\theta_\nu}{2})^2) \frac{d\alpha}{2}} \quad (\text{S16})$$

$$d \tan(\varphi_i) = -\frac{d\alpha \sin(\varphi_i)}{2 \cos(\varphi_i)^2} \left(\cot\left(\frac{\theta_i}{2}\right) - \tan\left(\frac{\theta_i}{2}\right)\right). \quad (\text{S17})$$

Using $d \tan(r) = (1 + \tan(r)^2)dr$

$$\frac{d\varphi_1}{d\alpha} = -\sin(\varphi_1) \left(\cot\left(\frac{\theta_1}{2}\right) - \tan\left(\frac{\theta_1}{2}\right)\right), \quad \frac{d\varphi_2}{d\alpha} = 0. \quad (\text{S18})$$

The remaining task to prove that $dd_{12}/d\alpha = 0$ is to derive $\xi_{1,2} = \arctan(q)$, where

$$q = \frac{\sin(\varphi_1)}{\cos(\varphi_1) + \cot(\frac{\theta_1}{2}) \cot(\frac{\theta_1}{2})} \quad (\text{S19})$$

To simplify the algebra we use the notation $c = \cos(\varphi_1)$, $s = \sin(\varphi_1)$ and $x_i = \cot(\theta_i/2)$. With this notation the equations (S14), (S15), (S18) and (S19) become

$$\frac{dx_1}{d\alpha} = -\frac{c}{2} (1 + x_1^2), \quad \frac{dx_2}{d\alpha} = -\frac{1}{2} (1 + x_2^2), \quad \frac{d\varphi_1}{d\alpha} = -\frac{s}{2} \left(x_1 - \frac{1}{x_1}\right), \quad q = \frac{s}{c + x_1 x_2} = \frac{s}{h}. \quad (\text{S20})$$

Differentiating the last expression we get

$$\frac{dq}{d\alpha} = \frac{c \frac{d\varphi_1}{d\alpha}}{h} - \frac{s \left(-s \frac{d\varphi_1}{d\alpha} + \frac{dx_1}{d\alpha} x_2 + x_1 \frac{dx_2}{d\alpha}\right)}{h^2} = \frac{\frac{d\varphi_1}{d\alpha} + c x_1 x_2 \frac{d\varphi_1}{d\alpha} - s \left(\frac{dx_1}{d\alpha} x_2 + x_1 \frac{dx_2}{d\alpha}\right)}{h^2} \quad (\text{S21})$$

and replacing Eqs. (S20) above, we obtain

$$\frac{dq}{d\alpha} = \frac{s}{2x_1} \frac{1 + 2cx_1x_2 + x_1^2x_2^2}{h^2} \quad (\text{S22})$$

On the other hand, from Eq. (S19)

$$\frac{d\xi_{1,2}}{d\alpha} = \frac{\frac{dq}{d\alpha}}{1 + q^2}, \text{ with } 1 + q^2 = 1 + \frac{s^2}{h^2} = \frac{1 + 2cx_1x_2 + x_1^2x_2^2}{h^2}, \quad (\text{S23})$$

and using Eq. (S22) we obtain

$$\frac{d\xi_{1,2}}{d\alpha} = \frac{s}{2x_1} = \frac{\sin(\varphi_1)}{2 \cot(\theta_1/2)}. \quad (\text{S24})$$

Finally, differentiating Eq. (S9) and expressing it as

$$\frac{dd_{12}}{d\alpha} = \frac{d\delta_1}{d\alpha} - \frac{d\delta_2}{d\alpha} + \frac{d\xi_{1,2}}{d\alpha}, \quad (\text{S25})$$

and substituting Eqs. (S11), (S19), and (S24) we get the desired result

$$\frac{dd_{12}}{d\alpha} = 0. \quad (\text{S26})$$

STRUCTURE OF THE MAJORANA STATES IN SOME LIMITING CASES

Solution for dominant spin-orbit coupling with $\vec{n}_B \equiv \vec{x}$ and $\vec{n}_\lambda \equiv \vec{z}$

We apply the formalism of Section to the exact solution of the continuum version of the model of Eq. (1) of the main text, calculated in Ref. [S1]. A very simple expression was found for the left and right MZMs in the region of parameters where the spin-orbit coupling dominates, assuming $\Delta > 0$, $\lambda \gg t$, $B > \Delta$, $\mu \sim 0$ (equivalent to $\mu \sim -2t$ in the lattice version). From there, we can easily examine the properties summarized in Eqs. (6) to (8) of the main text. The solution, as expressed in Ref. [S1] reads

$$\eta_L = \frac{1}{2} (\psi_{L,\uparrow} - i\psi_{L,\downarrow} + i\psi_{L,\downarrow}^\dagger + \psi_{L,\uparrow}^\dagger), \quad \eta_R = \frac{1}{2} (\psi_{R,\uparrow} + i\psi_{R,\downarrow} - i\psi_{R,\downarrow}^\dagger + \psi_{R,\uparrow}^\dagger), \quad (\text{S27})$$

where the labels L, R in the field operators indicate that they are evaluated at spacial coordinates corresponding the the L, R ends, respectively. In order to make an explicit comparison to Eqs. (7) and (8), we need to perform a rotation of $= \pi/2$ around the y -axis, corresponding to $\alpha = -\pi/2$ and $\vec{v} = (0, 1, 0)$ in Eq. (S2), and a change in the sign of λ which changes the sign of both δ and ϕ (see Ref. 53 of the main text). Under these transformations, the above operators transform to

$$\gamma'_L = e^{i\pi/4} (\psi'_{L,\uparrow} - i\psi'_{L,\downarrow}), \quad \gamma'_R = e^{-i\pi/4} (\psi'_{R,\uparrow} + i\psi'_{R,\downarrow}), \quad (\text{S28})$$

in full agreement with Eqs. (7) and (8) of the main text.

Solution for dominant magnetic field, $B \gg \Delta \gg \lambda$ with $\vec{n}_B \equiv \vec{z}$ and $\vec{n}_\lambda \equiv \vec{x}$

In this Section, we obtain analytically the zero-energy modes at the ends of a finite long chain for $0 < \lambda \ll \Delta \ll t < B$ and $\mu \sim -B$. We start with the Hamiltonian Eq. (9) of the main text, which to linear order in λ/B takes the form

$$H = \sum_{k,s=+,-} (-2t \cos k - \mu) d_{ks}^\dagger d_{ks} - B \sum_k (d_{k+}^\dagger d_{k+} - d_{k-}^\dagger d_{k-}) + \sum_k \left(\Delta_S d_{k+}^\dagger d_{-k-}^\dagger - \Delta_T \sin k \sum_{s=+,-} d_{ks}^\dagger d_{-ks}^\dagger + \text{H.c.} \right), \quad (\text{S29})$$

with $\Delta_S = \Delta$ and $\Delta_T = \lambda\Delta/B$. Transforming Fourier to Wannier functions localized at any site j , $d_{js}^\dagger = \sum_k e^{ijk} d_{ks}^\dagger / \sqrt{N}$, the Hamiltonian becomes

$$H = -t \sum_{j,s=+,-} (d_{js}^\dagger d_{j+1s} + \text{H.c.}) - B \sum_j (d_{j+}^\dagger d_{j+} - d_{j-}^\dagger d_{j-}) + \sum_j \left(\Delta_S d_{j+}^\dagger d_{j-}^\dagger + i\Delta_T \sum_{s=+,-} d_{j+1s}^\dagger d_{js}^\dagger + \text{H.c.} \right). \quad (\text{S30})$$

For later use we note that in the real-space basis, to linear order in λ/B the transformation introduced in the main text to define Eq. (9) from Eq. (1) reads

$$d_{j+}^\dagger = c_{j\uparrow}^\dagger - \frac{i\lambda}{2B} (c_{j+1\downarrow}^\dagger - c_{j-1\downarrow}^\dagger), \quad d_{j-}^\dagger = c_{j\downarrow}^\dagger + \frac{i\lambda}{2B} (c_{j+1\uparrow}^\dagger - c_{j-1\uparrow}^\dagger). \quad (\text{S31})$$

In order to eliminate the imaginary unit in the coefficient $i\Delta_T$ of the triplet superconductivity in Eq. (S30) we define

$$\tilde{d}_{j+}^\dagger = e^{i\pi/4} d_{j+}^\dagger, \quad \tilde{d}_{j-}^\dagger = e^{-i\pi/4} d_{j-}^\dagger \quad (\text{S32})$$

and the triplet superconducting term takes the form $\Delta_T \sum_j (\tilde{d}_{j+1+}^\dagger \tilde{d}_{j+}^\dagger - \tilde{d}_{j+1-}^\dagger \tilde{d}_{j-}^\dagger + \text{H.c.})$.

We obtain the solutions with zero energy of Eq. (S30) for a finite long chain of N sites using the method of Alase *et al.* [S2, S3] in the form used previously by some of us.[S4] As in the Nambu formalism, the operators are mapped to one particle states, using the following notation

$$\tilde{d}_{js} \leftrightarrow |js1\rangle, \quad \tilde{d}_{js}^\dagger \leftrightarrow |js2\rangle. \quad (\text{S33})$$

The desired solutions are linear combinations of states of the form (not normalized)

$$|zsi\rangle = \sum_{j=1}^N z^{j-1} |jsi\rangle, \quad s = \pm, \quad i = 1, 2, \quad (\text{S34})$$

where z is a complex number with $|z| < 1$ (> 1) for the Majorana zero mode localized at the left (right) of the chain. Since both modes are related by symmetry we focus here on the left mode only. The possible values of z are obtained from the bulk equation $P_B(H-E)|\psi\rangle = 0$, where in our case $E = 0$ and $P_B = \sum_{j=2}^{N-1} \sum_{si} |jsi\rangle\langle jsil|$. In the basis $|z, +, 1\rangle, |z, +, 2\rangle, |z, -, 1\rangle, |z, -, 2\rangle$, the matrix $P_B H$ takes the form

$$P_B H = \begin{pmatrix} -a & -b & 0 & \Delta_S \\ b & a & -\Delta_S & 0 \\ 0 & -\Delta_S & -a + 2B & b \\ \Delta_S & 0 & -b & a - 2B \end{pmatrix}, \quad a = \mu + B + t \left(z + \frac{1}{z} \right), \quad b = \Delta_T \left(z - \frac{1}{z} \right) \quad (\text{S35})$$

and its determinant is

$$\text{Det}(P_B H) = (a^2 - b^2) [(a - 2B)^2 - b^2] - [2a(2B - a) + 2b^2] \Delta_S^2 + \Delta_S^4. \quad (\text{S36})$$

To linear order in Δ_S/B , we can neglect Δ_S above and the four roots z_k of $\text{Det}(P_B H) = 0$ with $|z_k| < 1$ and the corresponding coefficients of the eigenvectors $|e_k\rangle = \sum_{si} \beta_{si}^k |jsi\rangle$, for $\mu' = \mu + B \ll t$ are

$$\begin{aligned} z_1 &= ic - \frac{\mu'}{2(t + \Delta_T)}, \quad \beta_{+1}^1 = \beta_{+2}^1 = \frac{1}{\sqrt{2}}, \quad \beta_{-1}^1 = \beta_{-2}^1 = 0, \quad c = \sqrt{\frac{t - \Delta_T}{t + \Delta_T}}, \\ z_2 &= \bar{z}_1 = -ic - \frac{\mu'}{2(t + \Delta_T)}, \quad \beta_{si}^2 = \beta_{si}^1, \\ z_3 &= \frac{2B - \mu'}{2(t + \Delta_T)} - \sqrt{\left(\frac{2B - \mu'}{2(t + \Delta_T)} \right)^2 - \frac{t - \Delta_T}{t + \Delta_T}}, \quad \beta_{+1}^3 = \beta_{+2}^3 = 0, \quad \beta_{-1}^3 = \beta_{-2}^3 = \frac{1}{\sqrt{2}}, \\ z_4 &= \frac{2B - \mu'}{2(t - \Delta_T)} - \sqrt{\left(\frac{2B - \mu'}{2(t - \Delta_T)} \right)^2 - \frac{t + \Delta_T}{t - \Delta_T}}, \quad \beta_{+1}^4 = \beta_{+2}^4 = 0, \quad -\beta_{-1}^4 = \beta_{-2}^4 = \frac{1}{\sqrt{2}}. \end{aligned} \quad (\text{S37})$$

The zero mode state has the form $|f\rangle = \sum_k \alpha_k |e_k\rangle$, and the coefficients are obtained from the boundary equation, which in our case takes the form $P_1 H |f\rangle = 0$, where $P_1 = \sum_{si} |1si\rangle\langle 1sil|$. It is easy to see that the form of the matrix $P_1 H$ is similar to Eq. (S35) without the terms in $1/z$ (due to the fact that there are no sites at the left of site 1), and z replaced by z_k . Taking for the basis state $|b\rangle$, the four states $|z, +, 1\rangle, |z, +, 2\rangle, |z, -, 1\rangle, |z, -, 2\rangle$, $\langle b | P_1 H | f \rangle = 0$ imply

$$\begin{aligned} \sum_k \left[-(\mu' + tz_k) \beta_{+1}^k - \Delta_T z_k \beta_{+2}^k + \Delta_S \beta_{-2}^k \right] \alpha_k &= 0, \\ \sum_k \left[\Delta_T z_k \beta_{+1}^k + (\mu' + tz_k) \beta_{+2}^k - \Delta_S \beta_{-1}^k \right] \alpha_k &= 0, \\ \sum_k \left[-\Delta_S \beta_{+2}^k + (2B - \mu' - tz_k) \beta_{-1}^k - \Delta_T z_k \beta_{-2}^k \right] \alpha_k &= 0, \\ \sum_k \left[\Delta_S \beta_{+1}^k + \Delta_T z_k \beta_{-1}^k - (2B - \mu' - tz_k) \beta_{-2}^k \right] \alpha_k &= 0. \end{aligned} \quad (\text{S38})$$

Using Eqs. (S37) and calling

$$C_{12} = \Delta_S (\alpha_1 + \alpha_2), \quad C_3 = 2B - \mu' - tz_3 - \Delta_T z_3, \quad C_4 = 2B - \mu' - tz_4 + \Delta_T z_4, \quad (\text{S39})$$

the last two Eq. (S38) can be written as

$$\begin{aligned} -C_{12} + C_3 \alpha_3 - C_4 \alpha_4 &= 0, \\ C_{12} - C_3 \alpha_3 - C_4 \alpha_4 &= 0. \end{aligned} \quad (\text{S40})$$

The solution of this equation is

$$\alpha_4 = 0, \quad \alpha_3 = \frac{C_{12}}{C_3}, \quad C_3 = B - \frac{\mu'}{2} + \sqrt{\left(B - \frac{\mu'}{2}\right)^2 - t^2 + \Delta_T^2}, \quad (\text{S41})$$

where the expression of C_3 has been obtained using Eqs. (S37) and (S39). From Eqs. (S37), (S39), and (S41) it is easy to see that the contribution of α_3 and α_4 to the first two Eqs. (S38) is either of order Δ_S^2 or zero. Therefore, it can be neglected to first order in Δ_S leading to

$$\sum_{k=1}^2 (\mu' + tz_k + \Delta_T z_k) \alpha_k = 0. \quad (\text{S42})$$

Using the expressions for z_k , the solution can be written in the form

$$\alpha_1 = \frac{e^{i\omega}}{\sqrt{2}}, \quad \alpha_2 = \frac{e^{-i\omega}}{\sqrt{2}}, \quad \omega = \arctan \left[\frac{(t + 2\Delta_T)\mu'}{2(t + \Delta_T)c} \right]. \quad (\text{S43})$$

Using $|f\rangle = \sum_k \alpha_k |e_k\rangle$, $|e_k\rangle = \sum_{si} \beta_{si}^k |jsi\rangle$, Eqs. (S32), (S33), (S34), (S37), (S41), and (S43), we obtain the final expression of the Majorana zero mode at the left end of the chain (except for a normalization factor)

$$\eta_L = \sum_{j=1}^N \left[\text{Re}(e^{i\omega} z_1^{j-1}) (e^{i\pi/4} d_{j+}^\dagger + e^{-i\pi/4} d_{j+}) + \frac{\Delta_S \cos \omega}{C_3} z_3^{j-1} (e^{-i\pi/4} d_{j-}^\dagger + e^{i\pi/4} d_{j-}) \right]. \quad (\text{S44})$$

The amplitude of the mode is maximum at the first site and decreases exponentially for sites inside the chain with different decay rates for spin + and -.

In order to make contact to Eqs. (7) and (8), we need to express η_L in terms of the operators $c_{j,\sigma}$ of the original model. To this end, we introduce the representation of Eqs. (S31) in to Eq. (S44) and focus on the limit $\lambda \rightarrow 0$. The projection of Eq. (S44) on the first site of the lattice reads $\eta_L = \gamma_L + \gamma_L^\dagger$ with

$$\gamma_L^\dagger \sim e^{i\pi/4} \left[c_{1,\uparrow}^\dagger + \frac{\Delta_S}{C_3} e^{-i\pi/2} c_{1,\downarrow}^\dagger \right]. \quad (\text{S45})$$

We see that this solution has the structure of Eq. (4) with

$$\delta_L = \pi/4, \quad \varphi_L = -\pi/2, \quad \tan(\theta_L/2) = \frac{\Delta_S}{C_3} + O\left(\frac{\lambda}{B}\right) \quad (\text{S46})$$

The results for δ_L and φ_L are valid for any value of the parameters in the topological phase with Δ , $t > 0$ and $\mu < 0$, with $\vec{n}_B \equiv \vec{z}$, $\vec{n}_\lambda \equiv \vec{x}$, and are in full agreement with the result of the continuum model discussed in Section . The value of θ_L is however very sensitive to the values of the parameters of the Hamiltonian. As explained in the main text, our goal is to show that this angle can be inferred from the behavior of the Josephson current in suitably designed junctions.

In contrast to δ_L and φ_L (obtained for $\vec{n}_B \parallel \vec{z}$ and $\vec{n}_\lambda \parallel \vec{x}$), θ depends on the site. As a consequence for other directions of \vec{n}_B and \vec{n}_λ (or other systems of coordinates), δ_L and φ_L also depend on the site, since their transformation properties depend on θ . Nevertheless for the calculation of the Josephson current we are only interested in the first and the last site of the chain.

NUMERICAL CALCULATION OF THE JOSEPHSON CURRENT

The Hamiltonian of the system describing two wires and a Josephson junction is

$$H(\phi) = H_{w1} + H_{w2} + H_c(\phi), \quad H_c = t_c \sum_{\sigma=\uparrow,\downarrow} \left(e^{i\phi/2} c_{1R,\sigma}^\dagger c_{2L,\sigma} + \text{H.c.} \right), \quad (\text{S47})$$

where H_{wi} , $i = 1, 2$, describe two topological superconducting wires, w1 at the left of w2, described by Eq. (1) of the main text, and with a difference $\phi = \phi_1 - \phi_2$ between the superconducting phases, with $\phi = 2\pi$ corresponding to one superconducting flux quantum. The subscript 1R (2L) indicates the last (first) site of w1 (w2). Denoting as $N_1 = \sum_{js} c_{1,js}^\dagger c_{1,js}$ the operator of total number of particles of w1, the current flowing through the junction from left to right is

$$J(\phi) = \left\langle e \frac{dN_L}{dt} \right\rangle = \left\langle \frac{ie}{\hbar} [N_1, H] \right\rangle = -\frac{et_c}{\hbar} \sum_{\sigma} \text{Im} \left[e^{i\phi/2} \left\langle c_{1R\sigma}^\dagger c_{2L\sigma} \right\rangle \right]. \quad (\text{S48})$$

The above expectation value can be numerically calculated given the eigenmodes of the Hamiltonian which correspond to annihilation operators that satisfy $[\Gamma_\nu, H] = \lambda_\nu \Gamma_\nu$, with positive λ_ν . The relevant part of these operators have the form

$$\Gamma_\nu = \sum_{\sigma} \left[A_{1R\sigma}^\nu c_{1R\sigma}^\dagger + A_{2L\sigma}^\nu c_{2L\sigma}^\dagger + B_{1R\sigma}^\nu c_{1R\sigma} + B_{2L\sigma}^\nu c_{2L\sigma} \right] + \dots, \quad (\text{S49})$$

where ... denotes the contribution of operators at site different from 1R and 2L. The coefficients are known from the numerical diagonalization. Inverting Eq. (S49) we have

$$c_{1R\sigma}^\dagger = \sum_{\nu} \left(\bar{A}_{1R\sigma}^\nu \Gamma_\nu + B_{1R\sigma}^\nu \Gamma_\nu^\dagger \right), \quad c_{2L\sigma} = \sum_{\nu} \left(A_{2L\sigma}^\nu \Gamma_\nu^\dagger + \bar{B}_{2L\sigma}^\nu \Gamma_\nu \right). \quad (\text{S50})$$

Replacing in Eq. (S48) and taking into account that in the ground state the only non vanishing expectation values of a product of two Γ_ν and/or Γ_ν^\dagger operators is $\langle \Gamma_\nu \Gamma_\nu^\dagger \rangle = 1$, we obtain

$$J(\phi) = -\frac{et_c}{\hbar} \text{Im} \left[e^{i\phi/2} \sum_{\nu\sigma} A_{2L\sigma}^\nu \bar{A}_{1R\sigma}^\nu \right]. \quad (\text{S51})$$

An alternative expression can be derived from the numerical derivative with respect of the flux of the eigenvalues λ_ν . This simplifies the diagonalization procedure at the cost of introducing numerical errors in the differentiation.

Noting that only H_c depends on the flux, Eq. (S48) can be also related to the ground state energy E_g as follows

$$J(\phi) = \frac{d\langle H \rangle}{d\phi} = \frac{t_c}{2} \sum_{\sigma} \left\langle i e^{i\phi/2} c_{1R,\sigma}^\dagger c_{2L,\sigma} + \text{H.c.} \right\rangle = \frac{2e}{\hbar} \frac{dE_g(\phi)}{d\phi}. \quad (\text{S52})$$

In turn, except for an additive constant, E_g can be calculated as half the sum of all positive eigenvalues of the Hamiltonian matrix $S = \sum_{\nu} \lambda_{\nu}$. The latter procedure can be justified by using symmetry arguments[S5] as follows. Considering the charge conjugation operation C , acting as $c_{i,j\sigma}^\dagger \leftrightarrow c_{i,j\sigma}$ plus complex conjugation. It is easy to see that $CHC = -H - 2\mu N$, where $N = N_1 + N_2$ is the total number of particles. Taking the number of particles as fixed $\langle N \rangle$, we can write this equation in the form $\tilde{H}' = CH'C = -H'$, $H' = H + \mu \langle N \rangle$, which can be considered as change of representation of the same states. Since both \tilde{H}' and H' have the same many-body spectrum but inverted, the maximum energy of H' , which we denote as E'_M and the ground state E'_g are related by $E'_M = -E'_g$. On the other hand the state of maximum energy is obtained applying all the creation operators Γ_ν^\dagger to the ground state. Therefore $E'_M - E'_g = S = \sum_{\nu} \lambda_{\nu}$, which leads to $E_g = -\frac{\sum_{\nu} \lambda_{\nu}}{2} - \mu \langle N \rangle$. Hence,

$$J(\phi) = -\frac{e}{\hbar} \frac{d \sum_{\nu} \lambda_{\nu}}{d\phi}. \quad (\text{S53})$$

We have verified that the results of Eq. (S51) and (S53) coincide within numerical precision.

NUMERICAL CALCULATION OF δ_ν , θ_ν AND φ_ν

The Majorana modes that enter the effective low-energy Hamiltonian H_{eff} for the Josephson current [see Eqs. (12) and (13) of the main text] have the form

$$\eta_\nu = \gamma_\nu^\dagger + \gamma_\nu, \quad \gamma_\nu^\dagger = a_\nu e^{i\delta_\nu} \left[\cos(\theta_\nu/2) c_{e\uparrow}^\dagger + e^{i\varphi_\nu} \sin(\theta_\nu/2) c_{e\downarrow}^\dagger \right] + \dots, \quad (\text{S54})$$

where a_ν is a real number that can be chosen positive, the subscript e refers to the site at the end of the chain (first or last) where the Majorana mode is localized and ... refers to the contribution of other sites which are not important for H_{eff} . The normalization $\eta_\nu^2 = 1$ implies that $a_\nu^2 \leq 1$ is the weight of the end site in the Majorana mode. Each fermionic operator γ_ν can be expressed as a

combination of two Majorana operators η_ν and $\tilde{\eta}_\nu$ of the form, $\gamma_\nu = (\eta_\nu + i\tilde{\eta}_\nu)/2$, $\gamma_\nu^\dagger = (\eta_\nu - i\tilde{\eta}_\nu)/2$, of which only η_ν contributes at low energy, $\gamma_\nu^\dagger \simeq \eta_\nu/2$.

For a finite chain, there is an effective mixing between the Majorana at the left (L) and right (R) end of the chain which by hermiticity should be proportional to $i\eta_L\eta_R$. Therefore, the one-particle eigenstates of lowest absolute value correspond to the fermions $f = e^{i\zeta}(\eta_L + i\eta_R)/2$ and f^\dagger which diagonalize $i\eta_L\eta_R$. The phase ζ is unknown. Thus, for the end we are interested (L or R) we can write, including explicitly only the operators related with that end

$$f = e^{i\zeta} \frac{\eta_\nu}{2} + \dots = Ac_{e\uparrow}^\dagger + Bc_{e\uparrow} + Cc_{e\downarrow}^\dagger + Dc_{e\downarrow} + \dots \quad (\text{S55})$$

where the coefficients at the right side are determined by the numerical calculation. Comparing with Eq. (S54) we see that the parameters of η_ν can be obtained from the following equations

$$a_\nu = 2\sqrt{(|A|^2 + |C|^2)}, \quad \delta_\nu = \frac{1}{2} \arctan\left(\frac{\text{Im}[A/B]}{\text{Re}[A/B]}\right), \quad \theta_\nu = 2 \arctan\left(\frac{|C|}{|A|}\right), \quad \varphi_\nu = \arctan\left(\frac{\text{Im}[C/A]}{\text{Re}[C/A]}\right). \quad (\text{S56})$$

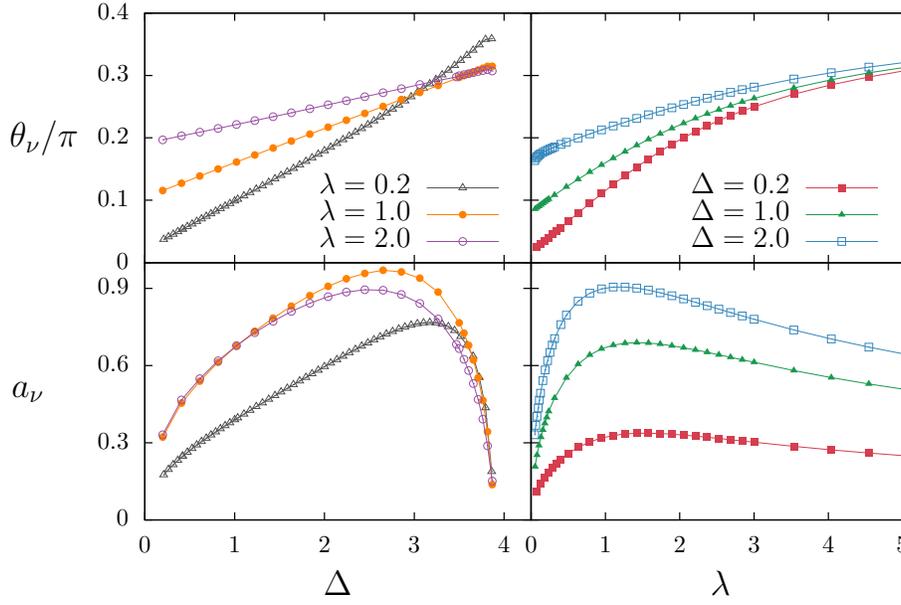


FIG. S1. Parameters θ_ν (top panels) and a_ν (bottom panels) as a function of Δ (λ) for several values of λ (Δ) and $t = 1$, $B = 4\mu = -3$, $\vec{n}_B \equiv \vec{z}$ and $\vec{n}_\lambda \equiv \vec{x}$.

The dependence of θ_ν and a_ν with the parameters, obtained numerically as described above is shown in Fig. S1. Both determine the coefficient t_J of the Josephson current. The amplitude a tends to zero at the borders of the topological region. Curiously, it has a maximum for intermediate values of λ . The angle θ tends to 0 or π (depending on the sign of $\vec{n}_B \cdot \vec{z}$) when both λ and Δ tend to zero as anticipated above.

As explained in the main text, for perpendicular directions of the magnetic field and spin-orbit coupling, δ_ν and φ_ν can be determined from symmetry arguments and analytical calculations. In particular, for $\vec{n}_B \parallel \vec{z}$ and $\vec{n}_\lambda \parallel \vec{x}$,

$$\delta_L = -\delta_R = \frac{\pi}{4}, \quad \varphi_L = -\varphi_R = -\frac{\pi}{2}. \quad (\text{S57})$$

In Fig. S2 we show how these parameters change when the orientation of the spin-orbit coupling \vec{n}_λ is rotated keeping it in the xy plane. We can see that the absolute values of δ_ν and φ_ν increase, keeping $\delta_L = -\delta_R$ and $\varphi_L = -\varphi_R$, as anticipated in the main text by symmetry arguments.

[S1] Y. Oreg, G. Refael, and F. von Oppen, Helical Liquids and Majorana Bound States in Quantum Wires, Phys. Rev. Lett. **105** 177002 (2010)

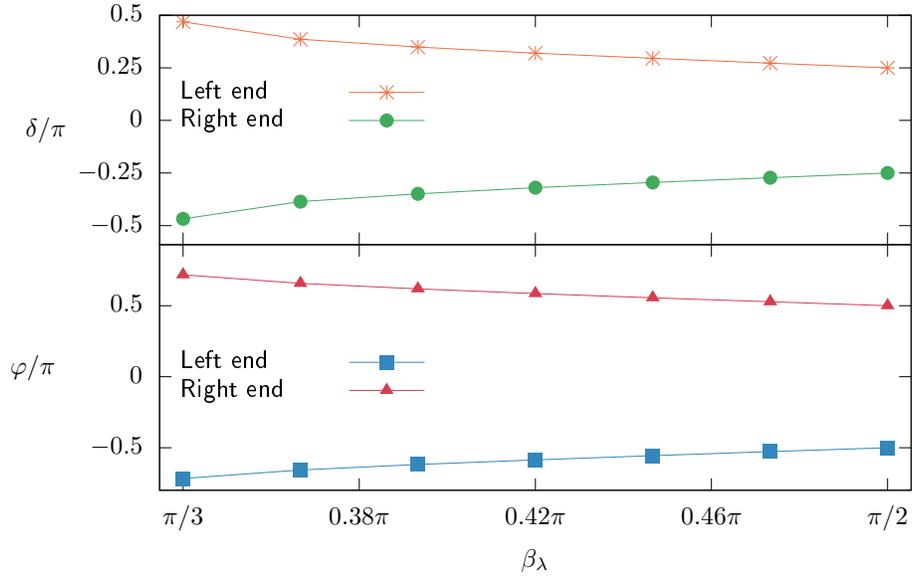


FIG. S2. Parameters δ_ν (top panel) and ϕ_ν (bottom panel) as a function of the angle between the magnetic field and spin-orbit coupling for $t = 1$, $B = 4$, $\Delta = \lambda = 2$, $\mu = -3$, $\vec{n}_\lambda \equiv \vec{x}$, and $\vec{n}_B \equiv \vec{z}$ in the xz plane.

- [S2] A. Alase, E. Cobanera, G. Ortiz, and L. Viola, Exact Solution of Quadratic Fermionic Hamiltonians for Arbitrary Boundary Conditions, *Phys. Rev. Lett.* **117**, 076804 (2016)
- [S3] A. Alase, E. Cobanera, G. Ortiz, and L. Viola, Generalization of Bloch's theorem for arbitrary boundary conditions: Theory, *Phys. Rev. B* **96**, 195133 (2017).
- [S4] A. A. Aligia and L. Arrachea, Entangled end states with fractionalized spin projection in a time-reversal-invariant topological superconducting wire, *Phys. Rev. B* **98**, 174507 (2018).
- [S5] A. A. Aligia and A. Camjayi, Exact analytical solution of a time-reversal-invariant topological superconducting wire, *Phys. Rev. B* **100**, 115413 (2019).
-